Benchmark: Extracting Table Information from Scientific Documents

BRGM Seminar

Marijan Soric

May 16, 2025

Outline

Project Context

Inria Valda (Inria Paris, DI ENS, CNRS) Topics: management of complex data, data generated by human activity

Inria Cedar (Inria Saclay, LIX, CNRS) Topics: Cloud-scale analysis of rich data

BRGM (*Bureau de Recherches Géologiques et Minières*) French National Geological Survey: Earth science applications for managing soil and subsoil resources and risks

Working environment

- GéolAug project collaboration Inria & BRGM
- Helping geologists prepare their missions, facilitating access to knowledge
- Thesis: "Exploitation and Structuring of Heterogeneous Geological Data and Knowledge"
- Heterogeneous data:
  - Geological maps, diagrams
  - Databases
  - Text
  - Tables

Outline

Definitions

Automatic structured table extraction from PDF documents

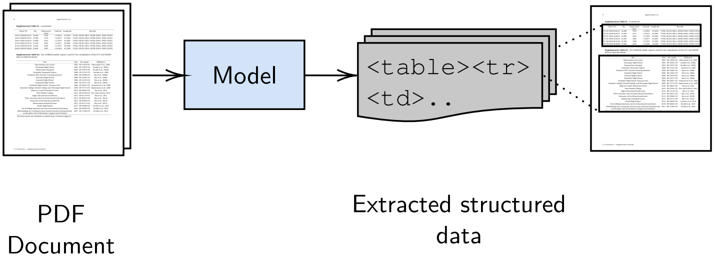

Task definition (1/2)

Table Detection: Find all tables within a document

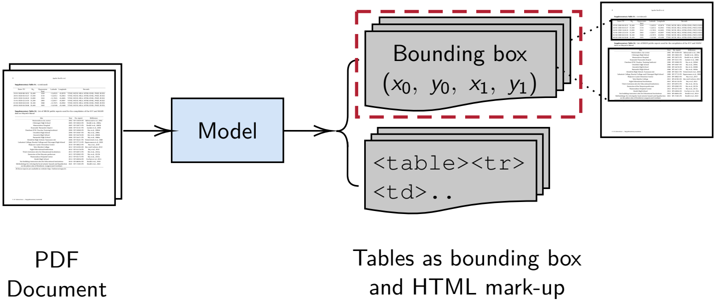

Hard: various table styles (with or without borders)

Task definition (2/2)

Table Structure Recognition: Extract content from tables while keeping their structures

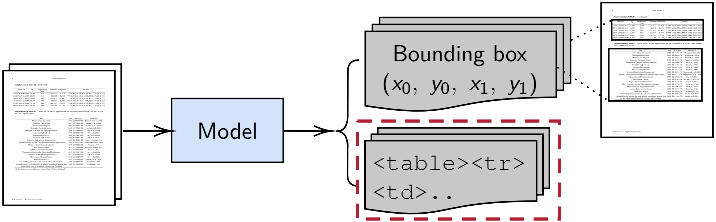

PDF Document

Tables as bounding box and HTML mark-up

Hard: various cell styles (empty, alignement. . .)

Table Extraction: Detection + Structure

Outline

Baseline

PdfPlumber	Python library, PDF parser, rule-based heuristics
Camelot	Python library, rule-based heuristics

Baseline

PdfPlumber	Python library, PDF parser, rule-based heuristics
Camelot	Python library, rule-based heuristics
GROBID	PDF parser, used in HAL https://hal.science

Baseline

PdfPlumber	Python library, PDF parser, rule-based heuristics
Camelot	Python library, rule-based heuristics
GROBID	PDF parser, used in HAL https://hal.science
LLM-Vision	GPT-4o-mini with OpenAI API

GROBID

GROBID (Lopez, 2008) PDF parser, used in HAL[1].

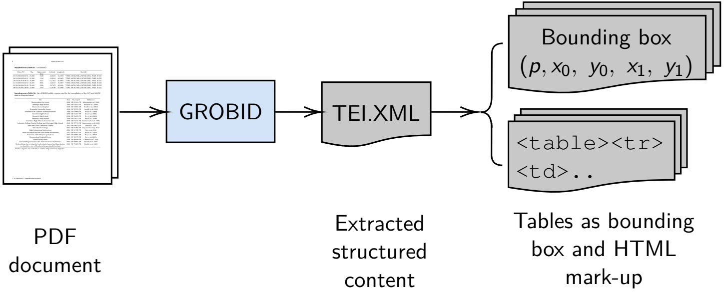

[1] https://hal.science

LLM-Vision

LLM-Vision GPT-4o-mini with OpenAI API

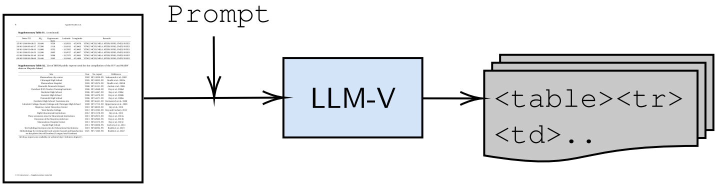

Page as an image

Tables as HTML mark-up

Note: LLM-Vision does not output coordinates

Outline

Object detection

Object detection: detect the instances in an image

Instance: Objet to find (“table”, “column”, “row”, “cell”).

Detection: Locations (bounding boxes) + probability distribution on labels (confiance score).

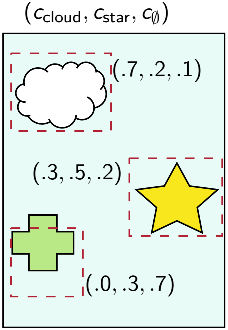

Object detection: instances (cloud, star, no object)

Baseline methods do not output confidence scores.

Two-step extraction method

Specialized models are assembled for each task.

Table Extraction Method	Table Detection	Table Structure Recognition
TATR-extract (Smock et al., 2022)	TATR-detect	TATR-structure
VGT+TATR-structure	VGT (Da et al., 2023)	TATR-structure
XY+TATR-extract	XY+TATR-detect	TATR-structure

Extraction method (1/3)

TATR-extract is composed of two models: TATR-detect and TATR-structure, using DETR (Carion et al., 2020) (transformer encoder-decoder) architecture.

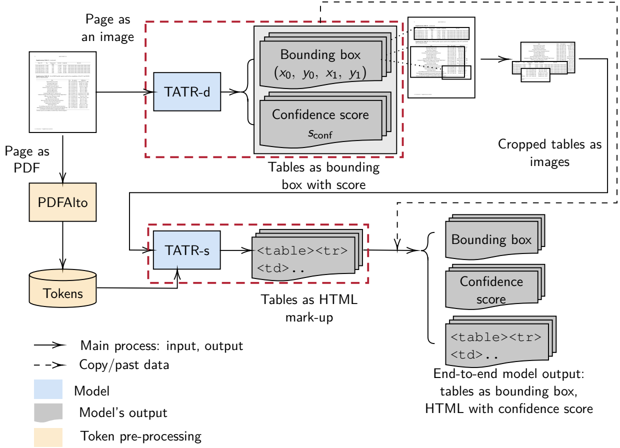

Extraction method (2/3)

VGT+TATR-structure uses VGT for table detection: specialized in document layout detection (including TD). VGT is multimodal: it operates on visual and textual content.

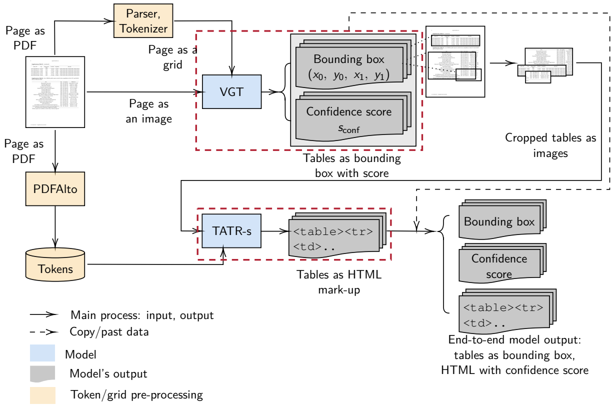

Extraction method (3/3)

XY+TATR-extract adds pre-processing with X-Y cut algorithm (Ha et al., 1995).

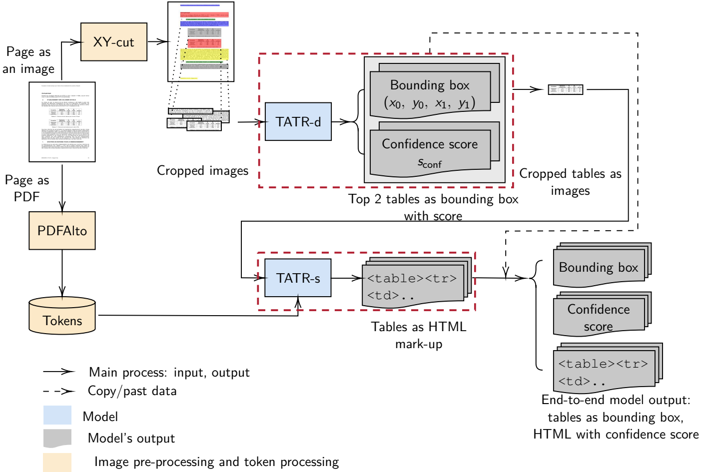

Outline

Table Detection

Usual metrics: Precision, Recall, based on *positive* predictions

Positive	"There is a table"
True Positive (TP)	Table correctly identified
False Positive (FP)	Detected table is not real
False Negative (FN)	True table not detected

$$P = \frac{TP}{TP + FP} \qquad R = \frac{TP}{TP + FN}$$

TP and FP (with bounding boxes)

We decide if a positive (prediction) is a TP or a FP using Intersection-over-Union (IoU) with a threshold θ_J.

$$\mathrm{IoU} = \frac{\text{area of overlap}}{\text{area of union}} =$$

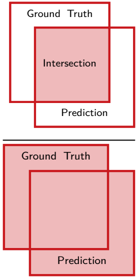

If $\mathrm{IoU} > \theta_J$ then the positive is a TP, otherwise a FP.

TP and FP (without bounding boxes)

We decide if a positive (prediction) is a TP or a FP using Jaccard-index according with a threshold θ_J.

$$\text{Jaccard}(S_P, S_{GT}) = \frac{|S_P \cap_{\text{multi}} S_{GT}|}{|S_P \cup_{\text{multi}} S_{GT}|}$$

Where S are multisets of 2-grams, where tokens are 2-characters (non-empty) strings from table content (HTML tags not included).

If $\mathrm{J} > \theta_J$ then the positive is a TP, otherwise a FP.

Metrics

Precision	P_{θ_J} mesures how precise the model is in its predictions
Recall	R_{θ_J} mesures how much the model misses real tables

But these metrics are sensitive to the choice of threshold θ_J, that is why we use metrics aggregating $\mathbb{E}_{\theta_J}[X_{\theta_J}]$ w.r.t $\theta_J \sim f$.

Average Precision	Area under the Precision–Recall curve for models with confidence scores.
Model miscalibration	Makes sure that confiance scores are probabilities.

Expected metrics

Before: binary value

$$TP^i = \mathbb{1}_{[\mathrm{IoU}_i > \theta_J]}$$

After: score

$$\widetilde{TP}^i = \mathbb{E}_{\theta_J}[\mathbb{1}_{[\mathrm{IoU}_i > \theta_J]}]$$

Expected metrics

Before: binary value

$$TP^i = \mathbb{1}_{[\mathrm{IoU}_i > \theta_J]}$$

After: score

$$\widetilde{TP}^i = \mathbb{E}_{\theta_J}[\mathbb{1}_{[\mathrm{IoU}_i > \theta_J]}]$$

Example:

$$\mathbb{E}_{\theta_J}[P_{\theta_J}] = \frac{1}{|\mathcal{P}|} \sum_{i \in \mathcal{P}} \mathbb{E}_{\theta_J}[\mathbb{1}_{[\mathrm{IoU}_i > \theta_J]}]$$

With $f(\theta_J) \propto \theta_J$ and $f(\theta_J) \propto \theta_J \mathbb{1}_{[0.5,1]}$

Outline

Table Structure Recognition

- Available metrics:
  - Structure absolute coordinates (rows, columns, cells) as we did for TD.
  - Cells relative positions and global structure, like TEDS (Li et al., 2020) and GriTS (Smock et al., 2023).
- Evaluation of extraction methods as a whole: the TSR part depends on the TD part.

Metrics (1/2)

TEDS measures the similarity of tables viewed as trees

<table>
<tr><th>Col.1</th><th>Col.2</th><th>Col.3</th></tr>
<tr><td>11</td><td rowspan="2">12-22</td><td>13</td></tr>
<tr><td>21</td><td>23</td></tr>
</table>

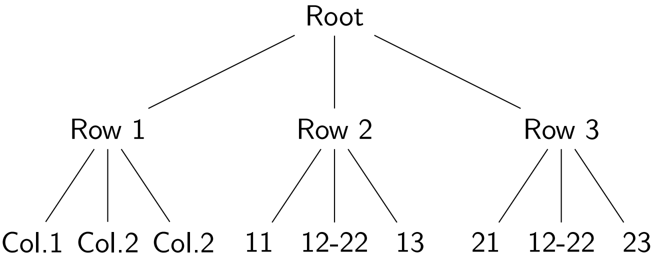

$$\mathrm{TEDS}(T_P, T_{GT}) = 1 - \frac{\mathrm{EditDist}(T_P, T_{GT})}{\max(|T_P|, |T_{GT}|)}$$

Metrics (2/2)

GriTS represents tables as matrices and computes different similarity types

GriTS Content

$$\begin{pmatrix} \text{Col.1} & \text{Col.2} & \text{Col.3} \\ 11 & 12-22 & 13 \\ 21 & 12-22 & 23 \end{pmatrix}$$

GriTS Topology

$$\begin{pmatrix} (0,0,1,1) & (0,0,1,1) & (0,0,1,1) \\ (0,0,1,1) & (0,0,1,2) & (0,0,1,1) \\ (0,0,1,1) & (0,-1,1,1) & (0,0,1,1) \end{pmatrix}$$

$$\mathrm{GriTS}_f(T_P, T_{GT}) = 2\frac{\sum_{i,j} f(\widetilde{T}_{P,i,j}, \widetilde{T}_{GT,j})}{|T_P| + |T_{GT}|}$$

With 2D most similar substructures $(\widetilde{T}_P, \widetilde{T}_{GT}) = \text{2D-MSS}_f(T_P, T_{GT})$

Outline

Table Extraction Metrics

Need to evaluate end-to-end methods on TE (not TD and TSR independently)
Before: binary value

$$TP^i = \mathbb{1}_{[\mathrm{IoU}_i > \theta_J]}$$

After: score

$$\widetilde{TP}^i = s_i^{\mathrm{TSR}} \mathbb{1}_{[\mathrm{IoU}_i > \theta_J]}$$

Table Extraction Metrics

Need to evaluate end-to-end methods on TE (not TD and TSR independently)
Before: binary value

$$TP^i = \mathbb{1}_{[\mathrm{IoU}_i > \theta_J]}$$

After: score

$$\widetilde{TP}^i = s_i^{\mathrm{TSR}} \mathbb{1}_{[\mathrm{IoU}_i > \theta_J]}$$

Finally,

$$P_{\theta_J}^{\mathrm{TSR}} = \frac{1}{|\mathcal{P}|} \sum_{i \in \mathcal{P}} s_i^{\mathrm{TSR}} \mathbb{1}_{[\mathrm{IoU}_i > \theta_J]}$$

$$R_{\theta_J}^{\mathrm{TSR}} = \frac{1}{|\mathcal{G}|} \sum_{i \in \mathcal{P}} s_i^{\mathrm{TSR}} \mathbb{1}_{[\mathrm{IoU}_i > \theta_J]}$$

Outline

Datasets

Table-BRGM manually annotated, PDF from geological reports from BRGM[2]

PubTables scientific articles from PubMed Central Open Access[3]

Table-arXiv synthetically generated from arXiv[4] paper source code. Use anchor and LaTeXML[5]

Dataset	# Pages	# Tables
Table-BRGM	499	124
PubTables	46 942	55 990
Table-arXiv	36 869	6 308

[2] https://infoterre.brgm.fr/rechercher/
[3] https://pmc.ncbi.nlm.nih.gov/tools/openftlist/
[4] https://arxiv.org
[5] http://dlmf.nist.gov/LaTeXML/

Outline

Confidence scores

Baseline: No confidence scores. $\mathcal{P}^+ = \mathcal{P}$. We can compute $P, R \ldots$

Object detection: With confidence scores. We have to define a set of positive predictions $\mathcal{P}^+_{\theta_c}$ from $\mathcal{P}$. We can then compute $P, R \ldots$

We use a threshold θ_c to define *positive* predictions from models with confidence scores.

$$\mathcal{P}^+_{\theta_c} := \{\widehat{y} \mid (\widehat{y}, c) \in \mathcal{P},\ c_{\text{table}} > \theta_c\}$$

Then we obtain tuples $\left(P^{\theta_c}, R^{\theta_c}\right)_{\theta_c}$

Precision–Recall curves with bounding boxes

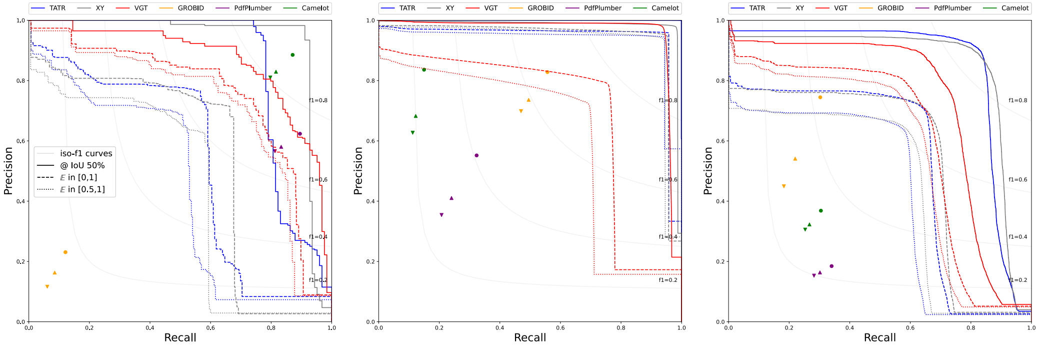

Figure: Table-BRGM, PubTables, Table-arXiv

Precision–Recall curves without bounding boxes

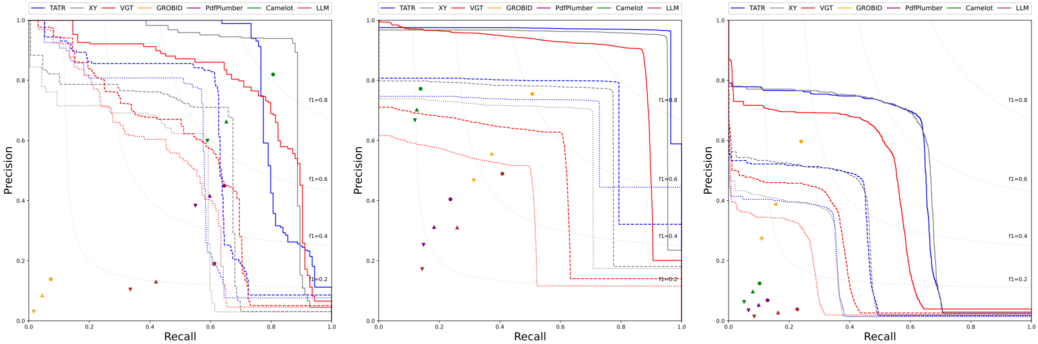

Figure: Table-BRGM, PubTables, Table-arXiv

Precision–Recall curves with bboxes (Table-BRGM)

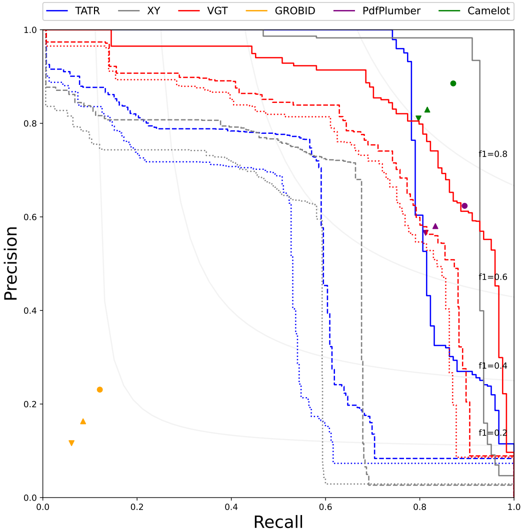

Precision–Recall curves with bboxes (PubTables)

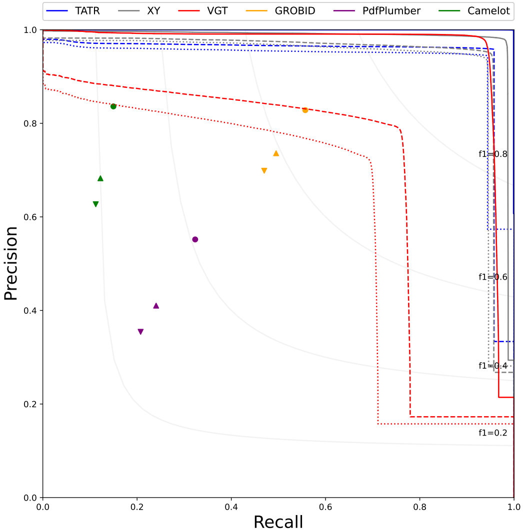

Precision–Recall curves with bboxes (Table-arXiv)

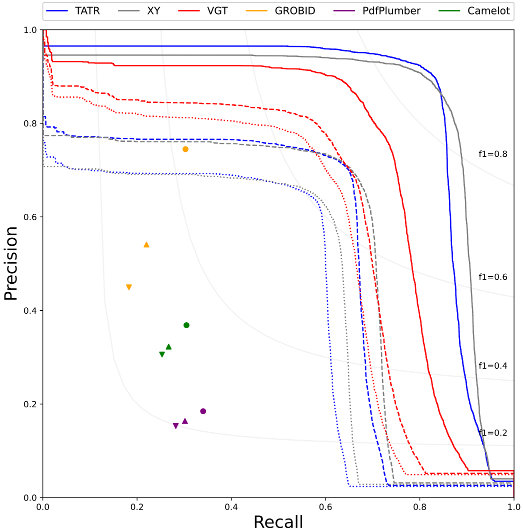

Example: comparison TATR-detect / VGT

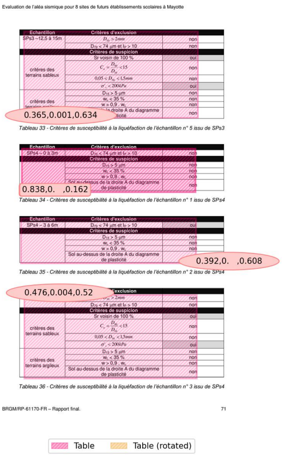

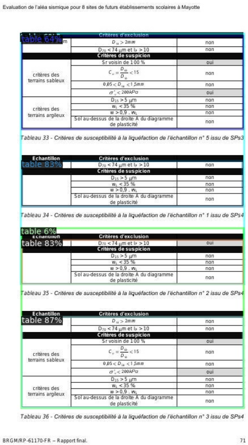

Model calibration

Should we trust confidence scores from models?

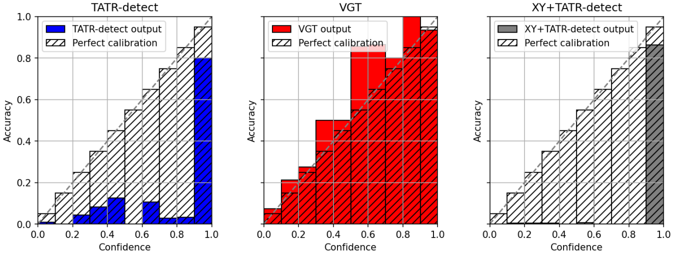

Reliability diagramms (Niculescu-Mizil & Caruana, 2005)

Outline

On which dataset should we evaluate TSR?

- The TSR part depends on the TD for evaluation.
- We decided to compute average TSR score on the set of *True Positive*: tuples (predicted table, ground truth table), setting with IoU @ 50%.

TSR histograms scores

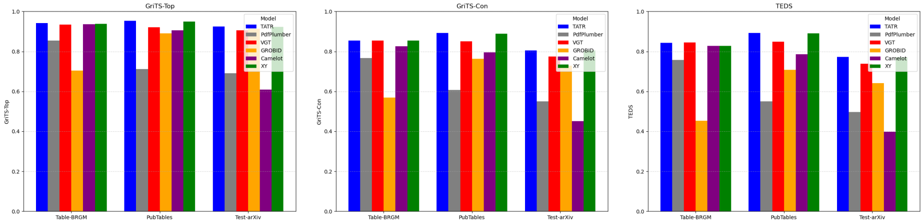

Figure: GriTS Topology, GriTS Content and TEDS.

Example: End-to-end extraction with TATR-extract

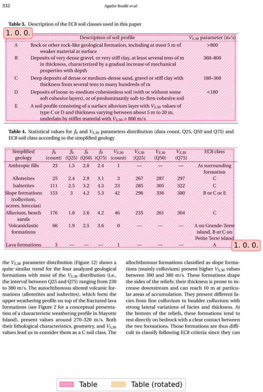

332 Agathe Roullé *et al.*

Table 3. Description of the EC8 soil classes used in this paper

Soil class	Description of soil profile	$V_{S,30}$ parameter (m/s)
A	Rock or other rock-like geological formation, including at most 5 m of weaker material at surface	>800
B	Deposits of very dense gravel, or very stiff clay, at least several tens of m in thickness, characterized by a gradual increase of mechanical properties with depth	360–800
C	Deep deposits of dense or medium-dense sand, gravel or stiff clay with thickness from several tens to many hundreds of m	180–360
D	Deposits of loose-to-medium cohesionless soil (with or without some soft cohesive layers), or of predominantly soft-to-firm cohesive soil	<180
E	A soil profile consisting of a surface alluvium layer with $V_{S,30}$ values of type C or D and thickness varying between about 5 m to 20 m, underlain by stiffer material with $V_{S,30}$ > 800 m/s	

Table 4. Statistical values for f_0 and $V_{S,30}$ parameters distribution (data count, Q25, Q50 and Q75) and EC8 soil class according to the simplified geology

Simplified geology	f_0 (count)	f_0 (Q25)	f_0 (Q50)	f_0 (Q75)	$V_{S,30}$ (count)	$V_{S,30}$ (Q25)	$V_{S,30}$ (Q50)	$V_{S,30}$ (Q75)	EC8 class
Anthropic fills	23	1.5	2.0	2.4	1	—	—	—	As surrounding formation
Alloterites	25	2.4	2.9	3.1	3	267	287	297	C
Isalterites	111	2.5	3.2	4.3	23	285	305	322	C
Slope formations (colluvium, screes, breccias)	153	3	4.2	5.3	42	296	336	380	B or C or E
Alluvium, beach sands	176	1.8	2.6	4.2	46	235	261	304	C
Volcaniclastic formations	66	1.9	2.5	3.6	0	—	—	—	A on Grande-Terre island, B or C on Petite Terre island
Lava formations	3	—	—	—	1	—	—	—	A

the $V_{S,30}$ parameter distribution (Figure 12) shows a quite similar trend for the four analyzed geological formations with most of the $V_{S,30}$ distribution (i.e., the interval between Q25 and Q75) ranging from 230 to 380 m/s. The autochthonous altered volcanic formations (alloterites and isalterites), which form the upper weathering profile on top of the fractured lava formations (see Figure 2 for a conceptual presentation of a characteristic weathering profile in Mayotte Island), present values around 270–320 m/s. Both their lithological characteristics, geometry, and $V_{S,30}$ values lead us to consider them as a C soil class. The allochthonous formations classified as slope formations (mainly colluvium) present higher $V_{S,30}$ values between 300 and 380 m/s. These formations drape the sides of the reliefs: their thickness is prone to increase downstream and can reach 10 m at particular areas of accumulation. They present different facies from fine colluvium to boulder colluvium with strong lateral variations of facies and thickness. At the bottom of the reliefs, these formations tend to rest directly on bedrock with a clear contact between the two formations. Those formations are thus difficult to classify following EC8 criteria since they can

(a) TATR-detect

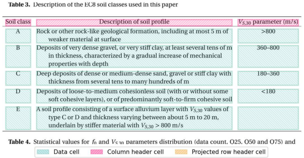

Table 3. Description of the EC8 soil classes used in this paper

Soil class	Description of soil profile	$V_{S,30}$ parameter (m/s)
A	Rock or other rock-like geological formation, including at most 5 m of weaker material at surface	>800
B	Deposits of very dense gravel, or very stiff clay, at least several tens of m in thickness, characterized by a gradual increase of mechanical properties with depth	360–800
C	Deep deposits of dense or medium-dense sand, gravel or stiff clay with thickness from several tens to many hundreds of m	180–360
D	Deposits of loose-to-medium cohesionless soil (with or without some soft cohesive layers), or of predominantly soft-to-firm cohesive soil	<180
E	A soil profile consisting of a surface alluvium layer with $V_{S,30}$ values of type C or D and thickness varying between about 5 m to 20 m, underlain by stiffer material with $V_{S,30}$ > 800 m/s	

Table 4. Statistical values for f_0 and $V_{S,30}$ parameters distribution (data count, Q25, Q50 and Q75) and

(b) TATR-structure

Soil class	Description of soil profile	V S,30 parameter (m/s)
A	Rock or other rock-like geological formation, including at most 5 m of weaker material at surface	>800
B	Deposits of very dense gravel, or very stiff clay, at least several tens of m in thickness, characterized by a gradual increase of mechanical properties with depth	360–800
C	Deep deposits of dense or medium-dense sand, gravel or stiff clay with thickness from several tens to many hundreds of m	180–360
D	Deposits of loose-to-medium cohesionless soil (with or without some soft cohesive layers), or of predominantly soft-to-firm cohesive soil	<180
E	A soil profile consisting of a surface alluvium layer with V S,30 values of type C or D and thickness varying between about 5 m to 20 m, underlain by stiffer material with V S,30 > 800 m/s	

(c) Extracted table (HTML)

Outline

TE Precision–Recall curves with bboxes (Table-BRGM)

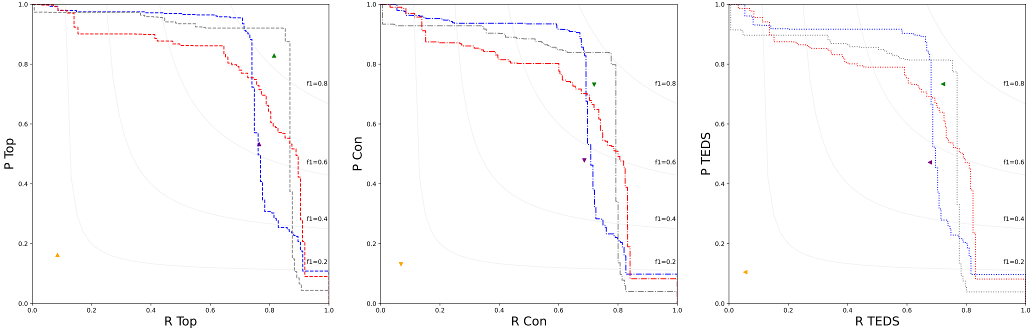

Figure: $P^{\mathrm{TSR}} - R^{\mathrm{TSR}}$ curves for GriTS Topology, GriTS Content and TEDS.

TE Precision–Recall curves with bboxes (PubTables)

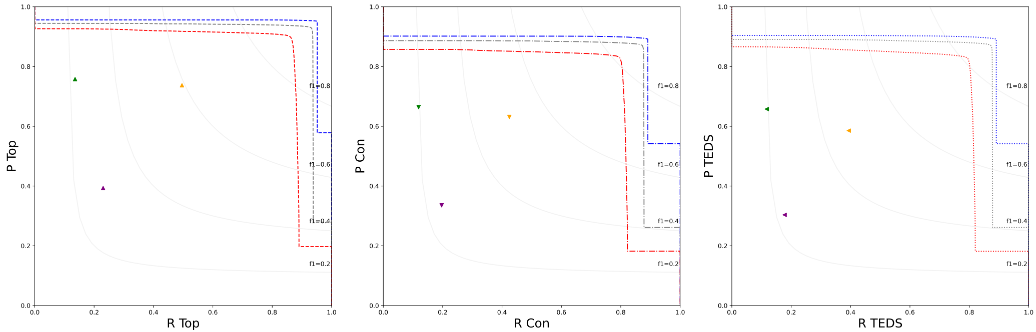

Figure: $P^{\mathrm{TSR}} - R^{\mathrm{TSR}}$ curves for GriTS Topology, GriTS Content and TEDS.

TE Precision–Recall curves with bboxes (Table-arXiv)

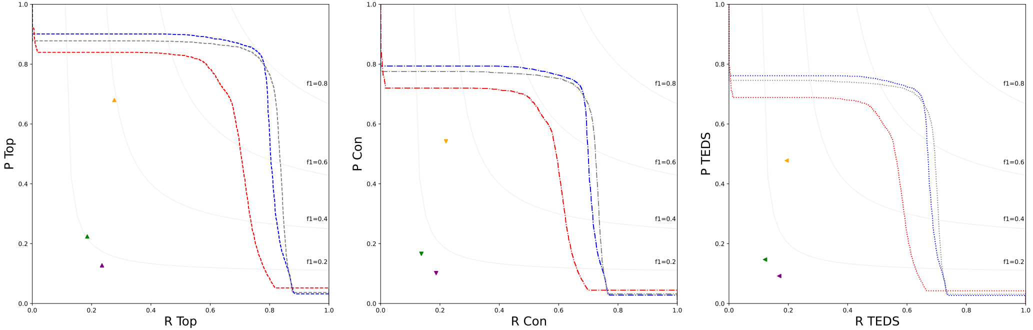

Figure: $P^{\mathrm{TSR}} - R^{\mathrm{TSR}}$ curves for GriTS Topology, GriTS Content and TEDS.

TE evaluation for models with scores

	Models	AP	$\mathrm{AP}^{\mathrm{Top}}$	$\mathrm{AP}^{\mathrm{Con}}$	$\mathrm{AP}^{\mathrm{TEDS}}$
BRGM	TATR	0.84	0.77	0.69	0.66
	VGT	0.86	0.76	0.67	0.65
	XY	**0.92**	**0.83**	**0.71**	**0.67**
PubTab	TATR	**1.00**	**0.91**	**0.80**	**0.80**
	VGT	0.96	0.81	0.69	0.70
	XY	0.97	0.88	0.78	0.78
arXiv	TATR	0.84	**0.73**	**0.56**	**0.52**
	VGT	0.73	0.60	0.44	0.40
	XY	**0.85**	**0.73**	**0.56**	0.51

TE evaluation for models without scores

	Models	F_1	F_1^{Top}	F_1^{Con}	F_1^{TEDS}
BRGM	Camelot	**0.88**	**0.82**	**0.73**	**0.73**
	GROBID	0.16	0.11	0.09	0.07
	PdfPlumber	0.73	0.63	0.56	0.56
PubTab	Camelot	0.25	0.23	0.20	0.20
	GROBID	**0.67**	**0.59**	**0.51**	**0.47**
	PdfPlumber	0.41	0.29	0.25	0.22
arXiv	Camelot	0.33	0.20	0.15	0.13
	GROBID	**0.43**	**0.39**	**0.31**	**0.28**
	PdfPlumber	0.24	0.17	0.13	0.12

Conclusion

- Problem not solved
- We developed new framework for TE evaluation, built datasets and compared various methods
- In downstream tasks, two choices:
  - Use a threshold θ_c in order to define $\mathcal{P}^+$
  - Trust confidence scores

Outlook

This work:

- Semantize tables through their content, context and captions
- Perform Q/A on tables

My thesis:

- Focus on other data types
- Exploite heterogeneous data through multi-modal methods
- Locate knowledge spatially and temporally

Carion, N., Massa, F., Synnaeve, G., Usunier, N., Kirillov, A., & Zagoruyko, S. (2020). End-to-end object detection with transformers. https://arxiv.org/abs/2005.12872

Da, C., Luo, C., Zheng, Q., & Yao, C. (2023). Vision grid transformer for document layout analysis. https://arxiv.org/abs/2308.14978

Ha, J., Haralick, R., & Phillips, I. (1995).Recursive x-y cut using bounding boxes of connected components. *Proceedings of 3rd International Conference on Document Analysis and Recognition*, *2*, 952–955 vol.2. https://doi.org/10.1109/ICDAR.1995.602059

- Li, M., Cui, L., Huang, S., Wei, F., Zhou, M., & Li, Z. (2020, May). TableBank: Table benchmark for image-based table detection and recognition. In N. Calzolari, F. Béchet, P. Blache, K. Choukri, C. Cieri, T. Declerck, S. Goggi, H. Isahara, B. Maegaard, J. Mariani, H. Mazo, A. Moreno, J. Odijk, & S. Piperidis (Eds.), *Proceedings of the twelfth language resources and evaluation conference* (pp. 1918–1925). European Language Resources Association. https://aclanthology.org/2020.lrec-1.236/
- Lopez, P. (2008). Grobid.
- Niculescu-Mizil, A., & Caruana, R. (2005).Predicting good probabilities with supervised learning. *Proceedings of the 22nd International Conference on Machine Learning*, 625–632. https://doi.org/10.1145/1102351.1102430
- Smock, B., Pesala, R., & Abraham, R. (2022).Pubtables-1m: Towards comprehensive table extraction from unstructured documents. *Proceedings of the IEEE/CVF Conference on Computer Vision and Pattern Recognition (CVPR)*, 4634–4642.

Smock, B., Pesala, R., & Abraham, R. (2023). Grits: Grid table similarity metric for table structure recognition. https://arxiv.org/abs/2203.12555